



OPEN ACCESS

EDITED BY

Jose Carlos Corchado,
University of Extremadura, Spain

REVIEWED BY

Krishanthi C. Weerasinghe,
Siena Heights University, United States
Juan Manuel Garrido-Zoido,
University of Extremadura, Spain

*CORRESPONDENCE

Yongjin Peng,
✉ pengyj@jzmu.edu.cn
Yuling Liu,
✉ liuy@jzmu.edu.cn

RECEIVED 06 June 2025

ACCEPTED 07 July 2025

PUBLISHED 23 July 2025

CITATION

Han H, Han B, Peng Y and Liu Y (2025) Decoding JFT: a multifunctional fluorescence probe for sulfite and viscosity insights.
Front. Chem. 13:1642191.
doi: 10.3389/fchem.2025.1642191

COPYRIGHT

© 2025 Han, Han, Peng and Liu. This is an open-access article distributed under the terms of the [Creative Commons Attribution License \(CC BY\)](#). The use, distribution or reproduction in other forums is permitted, provided the original author(s) and the copyright owner(s) are credited and that the original publication in this journal is cited, in accordance with accepted academic practice. No use, distribution or reproduction is permitted which does not comply with these terms.

Decoding JFT: a multifunctional fluorescence probe for sulfite and viscosity insights

Hua Han¹, Bin Han², Yongjin Peng^{3,4*} and Yuling Liu^{3,4*}

¹3rd Affiliated Hospital of Jinzhou Medical University, Jinzhou, China, ²Department of Physics, Tianjin Renai College, Tianjin, China, ³College of Modern Industry of Health Management, Jinzhou Medical University, Jinzhou, China, ⁴Liaoning Province Key Laboratory of Human Phenome Research, Jinzhou Medical University, Jinzhou, China

This study focuses on a multifunctional fluorescence probe JFT based on the FRET (Fluorescence Resonance Energy Transfer) and TICT (Twisted Intramolecular Charge Transfer) mechanism. JFT combines an electron donor and an acceptor, enabling it to detect sulfite and monitor intracellular viscosity. When reacting with sulfite, its electronic structure changes, turning off FRET and altering fluorescence wavelength and intensity. In different viscosity environments, the rotation of carbon-carbon bonds in the electron acceptor structure of JFT varies, affecting non-radiative transition pathways and fluorescence intensity. Theoretical calculations based on TDDFT reveal the electron distribution changes before and after the reaction with sulfite species, consistent with experimental phenomena. These findings deepen the understanding of the FRET mechanism of fluorescence probes and offer theoretical guidance for the design of more efficient fluorescence probes.

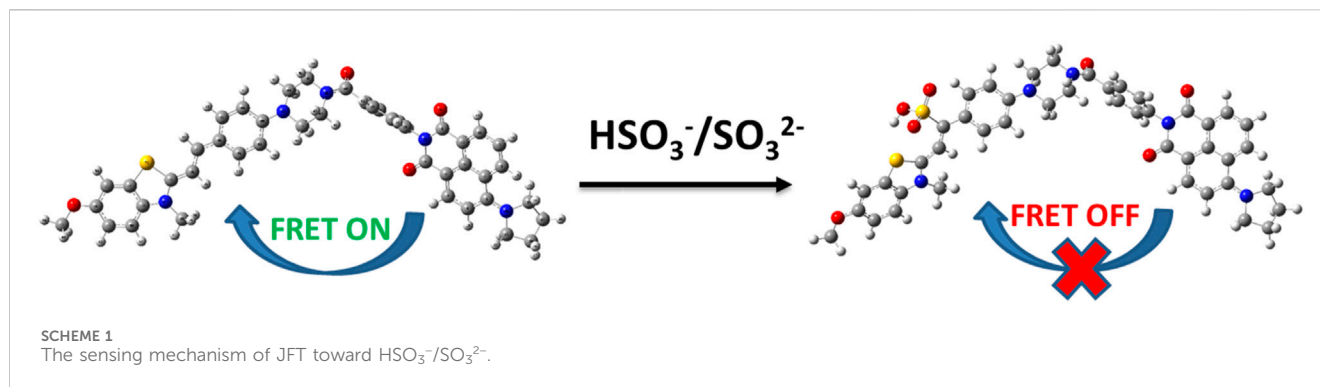
KEYWORDS

multifunctional, fluorescent probe, sulfite, intracellular viscosity, theoretical investigation

Introduction

Fluorescence probes have emerged as powerful tools in biological and chemical research, enabling real-time and non-invasive monitoring of various analytes and environmental parameters (Peng et al., 2024; Liu et al., 2024a; Liu et al., 2024b; Sun et al., 2019; Liu et al., 2024c). In the context of intracellular studies, simultaneously monitoring the changes in intracellular sulfite concentration and viscosity is of great significance. Sulfite is an important signaling molecule in the body, involved in many physiological and pathological processes, such as vasodilation, neurotransmission, and antioxidant defense (Zhang W. J. et al., 2022; Liu et al., 2023; Liu et al., 2022; Wang et al., 2024; Ren et al., 2024; Li et al., 2023). Abnormal levels of sulfite are associated with various diseases, including cardiovascular diseases, neurodegenerative diseases, and respiratory diseases. Therefore, accurately detecting the concentration of sulfite in cells is crucial for understanding its biological functions and related pathological mechanisms.

On the other hand, intracellular viscosity is a key physical parameter that reflects the micro-environment of cells. It affects many cellular processes, such as protein folding, enzyme activity, membrane fluidity, and intracellular transport. Changes in intracellular viscosity are often related to cell proliferation, differentiation, and apoptosis. Thus, monitoring intracellular viscosity can provide valuable information about cell status and



function (Peng et al., 2024; Liu et al., 2024c; Ma et al., 2024; Zhang C. et al., 2022; Arachchige et al., 2024; Wang et al., 2021; Peng et al., 2023).

However, developing a fluorescence probe that can simultaneously monitor these two parameters is challenging. Most traditional fluorescence probes are designed to detect only one analyte. The development of a multifunctional probe requires a careful combination of different sensing mechanisms.

Recently, Wang et al. developed a multifunctional fluorescence probe JFT based on the FRET/TICT mechanism (Wang et al., 2025). This probe effectively combined an electron donor and an acceptor, endowing it with unique properties for detecting sulfite and monitoring viscosity. The FRET property of the probe allowed for sensitive detection of sulfite through changes in fluorescence emission wavelength and intensity. Meanwhile, the rotation of carbon-carbon bonds in the electron acceptor structure of the probe was sensitive to environmental viscosity, enabling viscosity-dependent fluorescence changes. This paper aimed to comprehensively explore the working mechanism of the JFT fluorescence probe, including its response to sulfite and viscosity changes, as well as the underlying structural and electronic changes, which was expected to provide in-depth insights into fluorescence probe design and expand its applications in biological and chemical analysis.

Theoretical methods

The geometric optimization and vibrational frequency analysis on the probe JFT were carried out at the PBE0/def2-TZVPD level with D3 dispersion and GCP correction to remove artificial overbinding effects from BSSE using ORCA 5.0.1 program (Neese, 2022; Su et al., 2013; Laun and Bredow, 2022). To explore the excited-state properties of the molecule, the time-dependent density functional theory (TDDFT) computations were conducted at the CAM-B3LYP/def2-TZVPD level (Shao et al., 2020). The charges of the probe JFT and its reaction product with sulfite were +1 and 0 respectively. DMSO environment under the SMD solvent model was used in calculation which was align with the experimental work. All molecular visualizations were generated via the VMD 1.9.3 software, and the in-depth electronic structure analyses were accomplished by employing the Multiwfn 3.8 (dev) package (Lu and Chen, 2012; Humphrey et al., 1996).

Results and discussion

The emission spectrum of the electron donor of probe JFT could well overlap with the absorption spectrum of the acceptor of it, a characteristic that endowed the probe JFT with FRET properties. After the probe reacted with sulfite, the change in its electronic structure could turn off the FRET of probe JFT, thus causing significant changes in its fluorescence emission wavelength and intensity, making it an excellent sulfite detection probe. This mechanism was shown in Scheme 1.

Meanwhile, the electron acceptor structure in probe JFT contained C-C bonds with a high degree of rotational freedom. In a low-viscosity environment, these carbon-carbon bonds could rotate relatively freely, transferring energy among different conformations. This provided some non-radiative transition pathways for probe JFT to de-excite from the excited state to the ground state. When the environmental viscosity increased, the rotation of these carbon-carbon bonds was inhibited, and the non-radiative transition pathways for the probe to de-excite from the excited state to the ground state were cut off, thereby enhancing the corresponding fluorescence intensity. This enabled probe JFT to effectively monitor the intracellular viscosity level.

The structures of the JFT fluorescent probe and its electron donor and acceptor parts (same as Scheme 2 in Wang et al. (2025)) were shown in Figure 1. From the structural diagram of the electron acceptor part, it could be seen that the carbon-carbon bonds connecting the N-methylbenzothiazole and dimethylaniline had a large degree of rotational freedom, and the carbon-carbon double bond was also the reaction site with $\text{HSO}_3^-/\text{SO}_3^{2-}$. To study the rotational freedom of these carbon-carbon bonds, the compositional characteristics of the carbon-carbon bond in the probe JFT were analyzed through natural adaptive orbital concept and shown in Figure 2. The carbon-carbon bond had a relatively large proportion of easily rotatable σ component (70%), while the non-easily rotatable π component accounted for a relatively small proportion (28%).

To further study the conformational changes of the JFT fluorescence probe brought about by the rotation of these carbon-carbon bonds, the energy scan of the JFT probe's acceptor based on the rotation of these carbon-carbon bonds was carried out (Figure 3). It can be seen from Figure 3 that when N-methylbenzothiazole and dimethylaniline were in the same plane, the probe was in the lowest-energy conformation. When the carbon-carbon bond rotated to other angles, the probe was in other local low-energy conformations. The energy barriers between these conformations were relatively low. Therefore, in a low-viscosity environment, conversions between different conformations could occur relatively easily, providing a

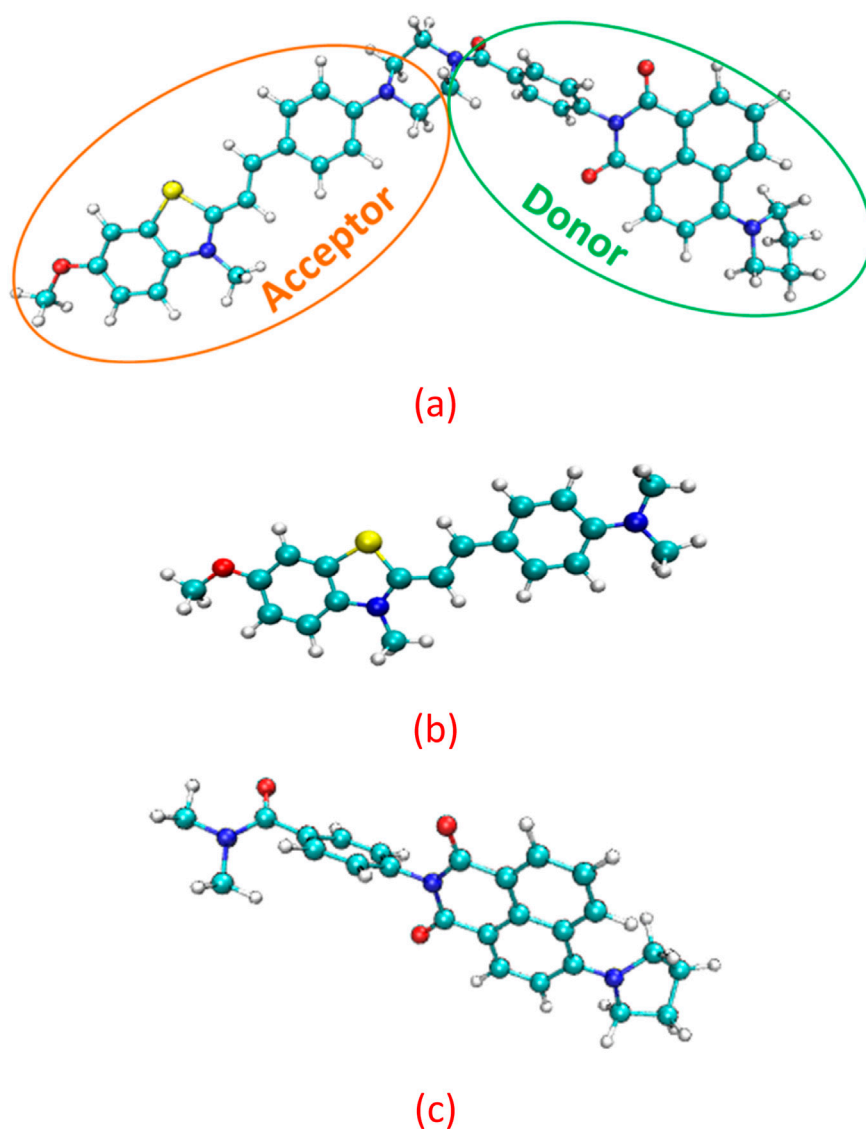


FIGURE 1
The structure of the (a) fluorescent probe JFT (b) acceptor (c) donor.

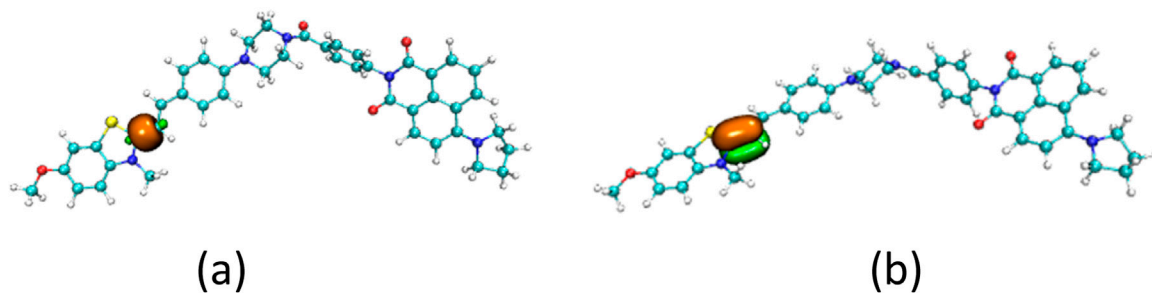


FIGURE 2
The σ component (a) and π component (b) of the c-c bond in probe JFT.

non-radiative energy dissipation path for the de-excitation of the JFT fluorescence probe, resulting in a weak fluorescence intensity of the JFT probe in this state. When the environmental viscosity increased, the

rotation of the carbon-carbon bonds in the probe was inhibited. When the JFT probe de-excited from the excited state back to the ground state, the fluorescence radiation path would be highly prioritized, thus causing

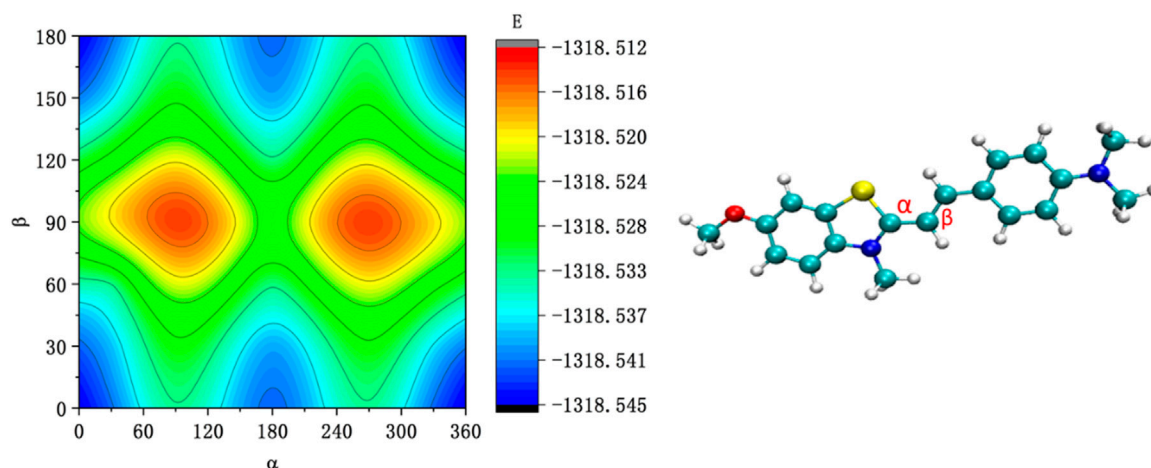


FIGURE 3
The energy scan of the JFT probe's acceptor based on the rotation of α and β carbon-carbon bonds.

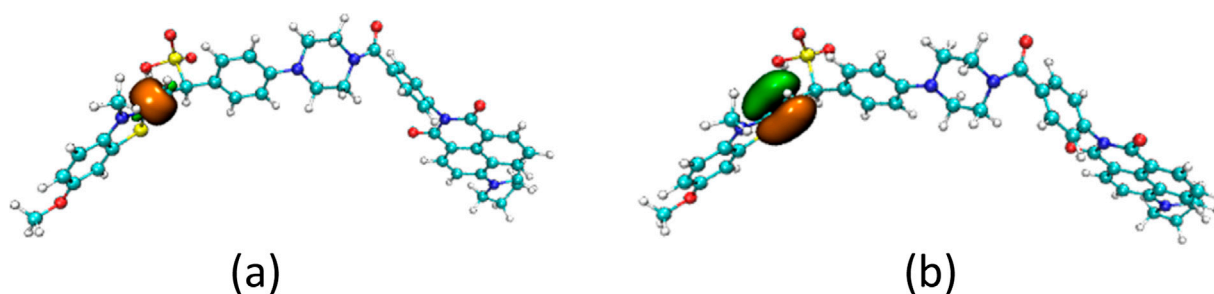


FIGURE 4
The σ component (a) and π component (b) of the c-c bond in product of JFT probe reacted with HSO_3^- .

a significant increase in fluorescence intensity. This conclusion was consistent with the experimental phenomena.

Another way to inhibit the rotation of the carbon-carbon bonds in probe JFT was that the composition of the carbon-carbon bonds was changed after the probe reacted with $\text{HSO}_3^-/\text{SO}_3^{2-}$. The proportion of rotatable σ component versus non-rotatable π component in the carbon-carbon bond changed from 70%:28%–57%:42% as shown in Figure 4. The addition of the HSO_3^- group significantly increased the inhibitory effect on the rotation of the carbon-carbon bonds, thereby also causing an enhancement in the fluorescence intensity of probe JFT under optical excitation.

At the same time, the introduction of the HSO_3^- group changed the electronic structure of the electron acceptor in probe JFT, so that the absorption spectrum of the changed acceptor no longer overlapped with the emission spectrum of its donor, thus cutting off the original FRET channel of the probe, as shown in Figure 5. This structural change caused significant changes in the fluorescence emission wavelength and intensity of probe JFT. The intensity of the original orange fluorescence (582 nm) was significantly weakened, while the intensity of the green fluorescence (530 nm) was significantly enhanced.

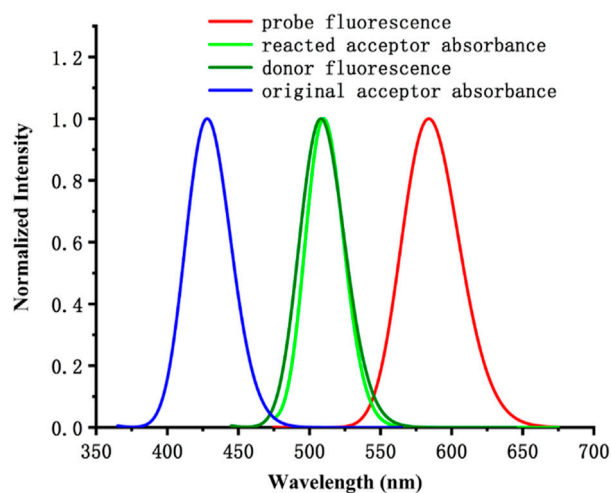


FIGURE 5
The calculated absorbance and fluorescence spectrum of the probe and its donor/acceptor.

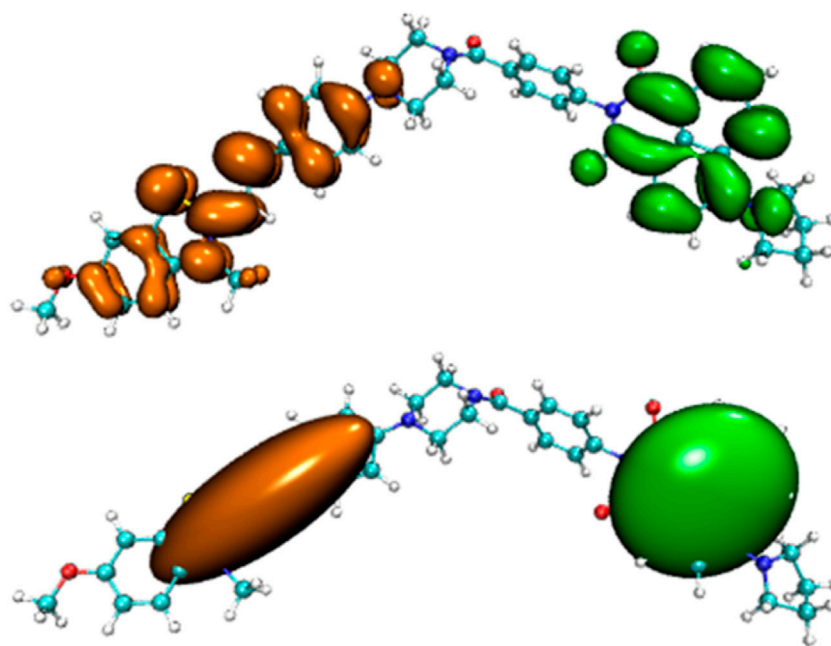


FIGURE 6
Difference diagram of electron distribution between S_0 and S_1 of probe JFT (orange:hole, green:electron).

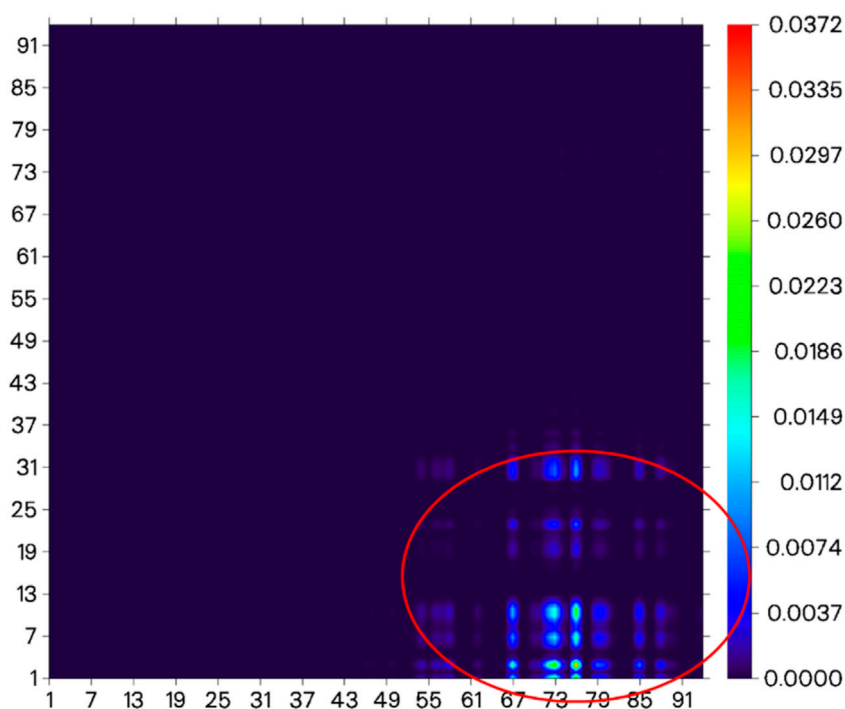


FIGURE 7
Electron-transfer heat map between S_0 and S_1 of probe JFT (donor part:1–31 to acceptor part:67–91 as shown in the red circle, the atom number list could be referenced to [Supplementary Figures S1, S2](#)).

Experimental results showed that there was a good linear relationship between the ratio I_{530}/I_{582} and the concentration of $\text{HSO}_3^-/\text{SO}_3^{2-}$ in the environment. Therefore, the fluorescence changed value I_{530}/I_{582} of probe JFT became an effective indicator

for monitoring the concentration of $\text{HSO}_3^-/\text{SO}_3^{2-}$ in the environment.

To further reveal the influence of the electronic structure changes of probe JFT before and after the reaction with $\text{HSO}_3^-/\text{SO}_3^{2-}$ on its

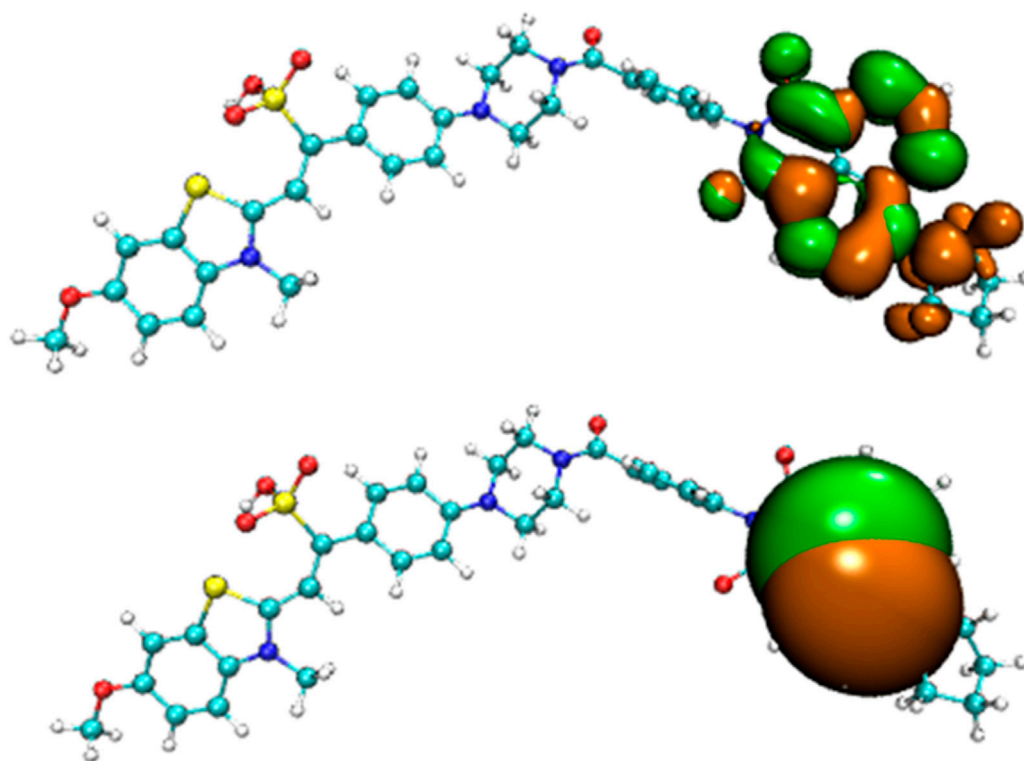


FIGURE 8
Difference diagram of electron distribution between S_0 and S_1 of the product of probe JFT reacted with HSO_3^- (orange:hole, green:electron).

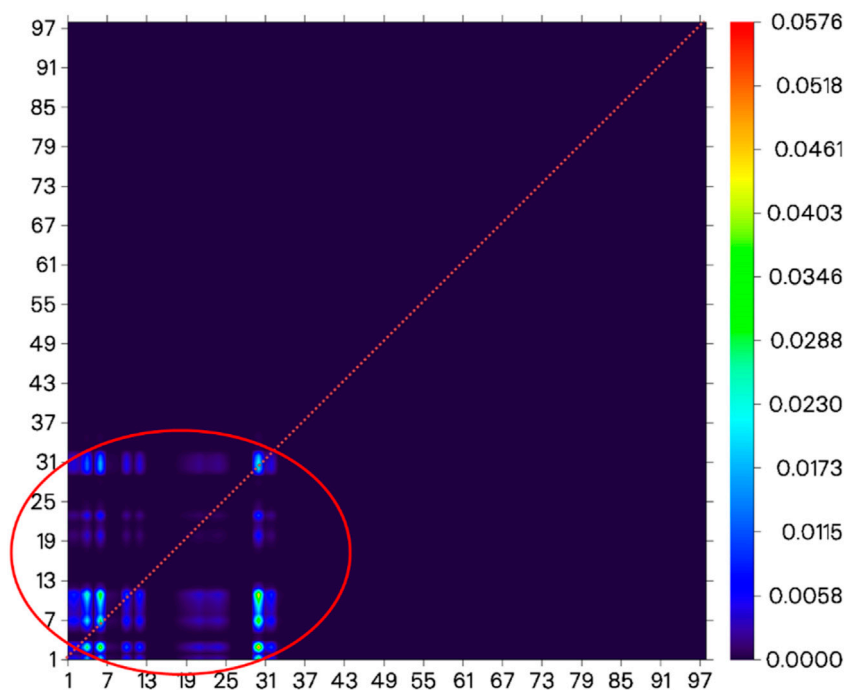


FIGURE 9
Electron-transfer heat map between S_0 and S_1 of the product of probe JFT reacted with HSO_3^- (donor part:1–31 to donor part:1–31 as shown in the red circle, the atom number list could be referenced to [Supplementary Figures S1, S2](#)).

TABLE 1 The main electron excitation processes in the JFT probe and its product reacting with $\text{HSO}_3^-/\text{SO}_3^{2-}$.

Probe	Electronic transition ^a	Excitation energy	Oscillator strength	Composition ^b	CI ^c
JFT	$S_0 \longrightarrow S_1$	408 nm	2.1804	$H \longrightarrow L$	0.7105
Donor	$S_0 \longrightarrow S_1$	403 nm	2.0042	$H \longrightarrow L$	0.6892
Acceptor	$S_0 \longrightarrow S_1$	426 nm	2.1465	$H \longrightarrow L$	0.6819
Product	$S_0 \longrightarrow S_1$	514 nm	2.1864	$H \longrightarrow L$	0.7014

^aOnly the excited states with oscillator strength larger than 0.1 were considered.^bH stand for HOMO and L stands for LUMO.^cCoefficient of the wave function for each excitation was in absolute value.TABLE 2 The main emission processes in the JFT probe and its product reacting with $\text{HSO}_3^-/\text{SO}_3^{2-}$.

Probe	Electronic transition ^a	Emission energy	Oscillator strength	Composition ^b	CI ^c
JFT	$S_1 \longrightarrow S_0$	578 nm	2.2046	$L \longrightarrow H$	0.7305
Donor	$S_1 \longrightarrow S_0$	503 nm	2.1121	$L \longrightarrow H$	0.6372
Acceptor	$S_1 \longrightarrow S_0$	561 nm	2.0437	$L \longrightarrow H$	0.6789
Product	$S_1 \longrightarrow S_0$	524 nm	2.1504	$L \longrightarrow H$	0.6914

a, b, c same indication as in Table 1.

fluorescence emission, the electron distribution of probe JFT in the ground state and excited state was studied based on the TDDFT method.

Before the reaction with $\text{HSO}_3^-/\text{SO}_3^{2-}$, the difference in electron distribution between the ground state S_0 and the first excited state S_1 of probe JFT showed obvious charge-transfer characteristics, which was consistent with the calculation results of the emission and absorption spectra of the probe's electron donor and acceptor as mentioned before. These characteristics could be clearly seen from the difference diagram of electron distribution between S_0 and S_1 as shown in Figure 6, and which atoms participate in the charge-transfer process could be further obtained from the electron-transfer heat map generated through Multiwfn program as shown in Figure 7. When probe JFT reacted with $\text{HSO}_3^-/\text{SO}_3^{2-}$, due to the change in the geometry and electronic structure of the electron acceptor, the FRET process was interrupted. The difference diagram of electron distribution between S_0 and S_1 of the product as shown in Figure 8 clearly showed the local excitation characteristics between the two states at this time, and the fluorescence color changed from orange (582 nm) to green (530 nm). Although due to the limitation of accuracy, there was some deviation within the calculated wavelength value from the experimental measurement value, the amplitude and trend of the wavelength change were in good agreement with the experiment. The difference diagrams of electron distribution between S_0 and S_1 and the electron-transfer heat map (Figure 9) both showed that electron excitation only occurred in the electron donor part of the probe at this time. The calculated results of the fluorescence emission wavelength were consistent with the experiment. The absorption and emission characteristic values of probe JFT before and after the reaction with $\text{HSO}_3^-/\text{SO}_3^{2-}$ and the corresponding donor and acceptor structure () were shown in Tables 1, 2 respectively. These theoretical results deepened our understanding of the FRET mechanism of fluorescence probes and provided theoretical inspiration for designing more efficient fluorescence probes based on these mechanisms in the future.

Conclusion

The development of the multifunctional fluorescence probe JFT represented a significant advancement in the field of fluorescence detection. Its ability to simultaneously monitor intracellular sulfite concentration and viscosity provided a powerful tool for studying related physiological processes. The combination of the FRET/TICT mechanism allowed the probe to respond sensitively to changes in sulfite levels and environmental viscosity. The clear understanding of the role of carbon-carbon bond rotation in fluorescence intensity regulation, as well as the influence of $\text{HSO}_3^-/\text{SO}_3^{2-}$ on the electronic structure and FRET process, provided a solid theoretical basis for the probe's performance. The good linear relationship between the fluorescence change value I_{530}/I_{582} and $\text{HSO}_3^-/\text{SO}_3^{2-}$ concentration demonstrated the probe's potential for quantitative detection. The TDDFT-based analysis of electron distribution further validated the experimental results and enriched the theoretical understanding of the probe's working mechanism. Overall, these results not only enhanced our knowledge of the FRET mechanism in fluorescence probes but also offer valuable theoretical inspiration for the future design of more efficient and sensitive fluorescence probes targeting similar biological parameters. However, further research could focus on improving the probe's accuracy, reducing the deviation between calculated and experimental values, and exploring its application in more complex biological systems.

Data availability statement

The original contributions presented in the study are included in the article/Supplementary Material, further inquiries can be directed to the corresponding authors.

Author contributions

HH: Data curation, Conceptualization, Formal analysis, Writing – review and editing. BH: Writing – review and editing, Data curation, Conceptualization. YP: Data curation, Writing – original draft, Conceptualization. YL: Conceptualization, Investigation, Writing – original draft.

Funding

The author(s) declare that no financial support was received for the research and/or publication of this article.

Conflict of interest

The authors declare that the research was conducted in the absence of any commercial or financial relationships that could be construed as a potential conflict of interest.

References

- Arachchige, D. L., Dwivedi, S. K., Olowolagba, A. M., Peters, J., Beatty, A. C., Guo, A., et al. (2024). Dynamic insights into mitochondrial function: monitoring viscosity and SO₂ levels in living cells. *J. Photoch Photobiol B* 258, 112986. doi:10.1016/j.jphotobiol.2024.112986
- Humphrey, W., Dalke, A., and Schulten, K. (1996). VMD: visual molecular dynamics. *J. Mol. Graph.* 14 (1), 33–38. doi:10.1016/02637855(96)000185
- Laun, J., and Bredow, T. (2022). BSSE-corrected consistent Gaussian basis sets of triple-zeta valence with polarization quality of the fifth period for solid-state calculations. *J. Comput. Chem.* 43 (12), 839–846. doi:10.1002/jcc.26839
- Li, Y., Wang, Y., Niu, H., Chen, X., Li, Z., and Wang, Y. (2023). Research progress of sulfur dioxide fluorescent probe targeting mitochondria. *Chin. J. Org. Chem.* 43 (6), 1952–1962. doi:10.6023/cjoc202210030
- Liu, F. T., Jiang, P. F., Wang, Y. P., Zhao, B. X., and Lin, Z. M. (2024a). A ratiometric fluorescent probe based on the FRET platform for the detection of sulfur dioxide derivatives and viscosity. *Anal. Chim. Acta* 1288, 342184. doi:10.1016/j.aca.2023.342184
- Liu, F. T., Wang, Y. P., Jiang, P. F., and Zhao, B. X. (2024c). A FRET-based ratiometric fluorescent probe for sensing bisulfite/sulfite and viscosity and its applications in food, water samples and test strips. *Food Chem.* 436, 137755. doi:10.1016/j.foodchem.2023.137755
- Liu, F. T., Zhai, S. M., Gao, D. F., Yang, S. H., Zhao, B. X., and Lin, Z. M. (2024b). A highly sensitive ratiometric fluorescent probe for detecting HSO₃[−]/SO₃^{2−} and viscosity change based on FRET/TICT mechanism. *Anal. Chim. Acta* 1305, 342588. doi:10.1016/j.aca.2024.342588
- Liu, P., Liu, Y. L., Huang, H., Bai, G., and Peng, Y. J. (2023). Theoretical investigation on FRET strategy of ratio metric fluorescent probe sensing hydrogen sulfide. *Spectrochim Acta A Mol Biomol Spectrosc* 289, 122223. doi:10.1016/j.saa.2022.122223
- Liu, Y. L., Huang, H., and Peng, Y. J. (2022). Fluorescent probe for simultaneous detection of human serum albumin and sulfite: a theoretical analysis. *J. Mol. Struct.* 1255, 132441. doi:10.1016/j.molstruc.2022.132441
- Lu, T., and Chen, F. W. (2012). Multiwfn: a multifunctional wavefunction analyzer. *J. Comput. Chem.* 33 (5), 580–592. doi:10.1002/jcc.22885
- Ma, J. Y., Zhao, M. T., Qin, C., Kong, X. T., Xie, H., Zhang, X. S., et al. (2024). An oxidizer-resistant fluorescence probe for detecting bisulfite and viscosity in biosystems. *Dyes Pigments* 229, 112321. doi:10.1016/j.dyepig.2024.112321
- Neese, F. (2022). Software update: the ORCA program system-Version 5.0. *Wires Comput. Mol. Sci.* 12 (5). doi:10.1002/wcms.1606
- Peng, Y. J., Huang, H., Liu, Y. L., and Zhao, X. Y. (2023). Theoretical insights into a near-infrared fluorescent probe NI-VIS based on the organic molecule for

Generative AI statement

The author(s) declare that no Generative AI was used in the creation of this manuscript.

Publisher's note

All claims expressed in this article are solely those of the authors and do not necessarily represent those of their affiliated organizations, or those of the publisher, the editors and the reviewers. Any product that may be evaluated in this article, or claim that may be made by its manufacturer, is not guaranteed or endorsed by the publisher.

Supplementary material

The Supplementary Material for this article can be found online at: <https://www.frontiersin.org/articles/10.3389/fchem.2025.1642191/full#supplementary-material>

monitoring intracellular viscosity. *Molecules* 28 (16), 6105. doi:10.3390/molecules28166105

Peng, Z. X., Zhang, D., Yang, H., Zhou, Z., Wang, F. Y., Wang, Z., et al. (2024). Mitochondria-targeted fluorescent probe for simultaneously imaging viscosity and sulfite in inflammation models. *Analyst* 149 (12), 3356–3362. doi:10.1039/d4an00467a

Ren, J., Zhang, W., Gao, X., Song, B., and Yuan, J. (2024). Unveiling the negative correlation of formaldehyde and hydrogen sulfide in Parkinson's disease models using a dual-responsive ruthenium(II) complex probe. *Chem. Eng. J.* 486, 150349. doi:10.1016/j.cej.2024.150349

Shao, Y. H., Mei, Y., Sundholm, D., and Kaila, V. R. I. (2020). Benchmarking the performance of time-dependent density functional theory methods on biochromophores. *J. Chem. Theory Comput.* 16 (1), 587–600. doi:10.1021/acs.jctc.9b00823

Su, N. Q., Adamo, C., and Xu, X. (2013). A comparison of geometric parameters from PBE-based doubly hybrid density functionals PBE0-DH, PBE0-2, and xDH-PBE0. *J. Chem. Phys.* 139 (17), 174106. doi:10.1063/1.4827024

Sun, C., Cao, W. F., Zhang, W., Zhang, L. L., Feng, Y., Fang, M., et al. (2019). Design of a ratiometric two-photon fluorescent probe for dual-response of mitochondrial SO₂ derivatives and viscosity in cells and *in vivo*. *Dyes Pigments* 171, 107709. doi:10.1016/j.dyepig.2019.107709

Wang, J. F., Cui, X. L., Lun, S. H., Yang, D., Gao, C., Zhang, K. Y., et al. (2025). A FRET/TICT based multifunctional fluorescent probe for the monitoring of SO₂ derivatives and viscosity in living cells and real samples. *Spectrochim Acta A Mol Biomol Spectrosc* 325, 125074. doi:10.1016/j.saa.2024.125074

Wang, X., Tang, H., and Huang, X. H. (2021). Water-soluble fluorescent probes for bisulfite and viscosity imaging in living cells: pyrene vs. anthracene. *Spectrochim Acta A Mol Biomol Spectrosc* 260, 119902. doi:10.1016/j.saa.2021.119902

Wang, X., Zhou, X., Li, C., Qu, C., Shi, Y., Li, C.-J., et al. (2024). Integrative analysis of whole genome bisulfite and transcriptome sequencing reveals the effect of sodium butyrate on DNA methylation in the differentiation of bovine skeletal muscle satellite cells. *Genomics* 116 (6), 110959. doi:10.1016/j.ygeno.2024.110959

Zhang, C., Li, J. R., Chen, X. L., Hu, Y. J., and Huang, X. H. (2022). Rational design of ratiometric fluorescent probes for bisulfite and viscosity detection in mitochondria without spectral crosstalk. *Dyes Pigments* 207, 110666. doi:10.1016/j.dyepig.2022.110666

Zhang, W. J., Lv, Y. X., Song, H. J., Huo, F. J., Zhang, Y. B., and Yin, C. X. (2022). Biological roles of sulfur dioxide and sulfite in the regulation of mitochondrial viscosity. *Chem. Commun.* 58 (61), 8524–8527. doi:10.1039/d2cc03420d